A Comparison of Chaotic Electromagnetic Field Optimization Algorithms

Olympia Roeva[1], **Dafina Zoteva**[2*]

[1]*Department of Bioinformatics and Mathematical Modelling*
Institute of Biophysics and Biomedical Engineering
Bulgarian Academy of Sciences
Acad. G. Bonchev Str., bl. 105, 1113 Sofia, Bulgaria
E-mail: olympia@biomed.bas.bg

[2]*Department of Computer Informatics*
Faculty of Mathematics and Informatics
Sofia University "St. Kliment Ohridski"
5 James Bourchier Blvd., 1164 Sofia, Bulgaria
E-mail: dafinaz@fmi.uni-sofia.bg

[*]*Corresponding author*

Received: March 09, 2023 **Accepted: November 07, 2023**

Published: December 31, 2024

Abstract: *This paper investigates the performance of various Electromagnetic Field Optimization (EFO) algorithms. Chaos maps are proposed to improve the performance of EFO algorithms. Ten chaotic maps are incorporated in EFO – Chebyshev, Circle, Gauss, Iterative, Logistic, Piecewise, Sine, Singer, Sinusoidal and Tent. To compare the performance of the constructed EFO algorithms, a case study of the identification of the model parameters of a cultivation process model is studied. An experimental data set from E. coli BL21(DE3)pPhyt109 fed-batch cultivation process is used. Based on the results of 30 runs of each EFO, some statistical and InterCriteria analyzes are performed. As a result, the best performing EFO algorithms are iterative EFO and tent chaotic map EFO. These algorithms gave the best objective value (best and mean value) and had a good distribution of results.*

Keywords: *Chaotic maps, Electromagnetic field optimization, InterCriteria analysis, E. coli BL21(DE3)pPhyt109 fed-batch cultivation.*

Introduction

Metaheuristic algorithms, such as the Genetic algorithm, Particle Swarm Intelligence, Artificial Bee Colony, etc. have been effectively employed to various complex tasks. Among the existing metaheuristic algorithms, the Electromagnetic field optimization (EFO) [1] is a promising algorithm, inspired by the behavior of electromagnets with different polarities and takes advantage of a nature-inspired ratio, known as the golden ratio.

EFO algorithm has been applied in several areas [19, 30, 34, 38, 41, 48]. There are published same improvements of the EFO [2–5, 49]. In the literature some results of improved EFO are based on chaotic maps [17, 21, 24, 39, 40]. In the paper [39], an effective technique of EFO algorithm based on a fuzzy entropy criterion is proposed, and in addition, a novel chaotic strategy is embedded into EFO. A series of experiments significantly demonstrate the superior performance of the proposed technique. Bouchekara [17] developed an improved version of EFO based on chaotic maps and on a new mechanism. The obtained results are compared with other well-known algorithms and show the ability of the improved EFO to solve efficiently different problems. An improved diversification step with chaos in EFO is presented in [24]. The obtained results are compared with the results from other recent and improved algorithms in the literature to show the performance and effectiveness of the proposed algorithm. Two nonparametric statistical tests, the Wilcoxon rank-sum and the Friedman test, are performed to

determine the significance of the results. Here, InterCriteria Analysis (ICrA) is applied instead of well-known statistical tests.

ICrA has been developed with the goal to gain additional insight into the nature of criteria involved in a multicriteria problem, and discover on this basis existing relations between the criteria themselves [9]. It is based on the apparatus of the Index Matrices (IM) [7], and the Intuitionistic Fuzzy Sets (IFS) [6, 8] and can be applied to decision making in different areas of knowledge.

The approach has been discussed in details in a number of papers devoted to different areas of application [20, 44] and still finds scientific interest [18, 22, 45, 46]. In this paper ICrA has been applied to compare the numerical results from EFO algorithm with 10 different chaotic maps [20]. Ten different chaotic maps are incorporated into the EFO, namely, Chebyshev, Circle, Gauss, Iterative, Logistic, Piecewise, Sine, Singer, Sinusoidal and Tent. The ten EFO algorithms are applied to a model parameter identification problem of a non-linear *E. coli* fed-batch cultivation process. Cultivation processes are characterized with complex, non-linear dynamic and their modelling is a hard combinatorial optimization problem. *E. coli* is still the most important host organism for recombinant protein production [47]. Cultivation of recombinant micro-organisms e.g. *E. coli*, in many cases is the only economical way to produce pharmaceutical biochemicals such as interleukins, insulin, interferons, enzymes and growth factors. Simple bacteria like *E. coli* are manipulated to produce these chemicals so that they are easily harvested in vast quantities for use in medicine. As a case study, *E. coli* BL21(DE3)pPhyt109 fed-batch cultivation for bacterial phytase extracellular production [36] is used.

The rest of the paper is organized as follows. In Sections 2, 3 and 4 the InterCriteria Analysis, Chaos theory and EFO background are presented, respectively. In Section 5 the used test case, model parameter identification of an *E. coli* BL21(DE3)pPhyt109 fed-batch cultivation process, is presented. Section 6 shows numerical results and discussion. Conclusions and directions for future work are done in Section 7.

InterCriteria analysis

InterCriteria analysis, based on the apparatuses of IM [10–12] and IFS [6, 14], is given in details in [9]. Here, for completeness, the proposed idea is briefly presented.

Let the initial IM is presented in the form of Eq. (1), where, for every p, q, $(1 \leq p \leq m, 1 \leq q \leq n)$, C_p is a criterion, taking part in the evaluation; O_q – an object to be evaluated; $C_p(O_q)$ – a real number (the value assigned by the p-th criteria to the q-th object).

$$A = \begin{array}{c|ccccc} & O_1 & \ldots & O_q & \ldots & O_n \\ \hline C_1 & C_1(O_1) & \ldots & C_1(O_q) & \ldots & C_1(O_n) \\ \vdots & \vdots & \ddots & \vdots & \ddots & \vdots \\ C_p & C_p(O_1) & \ldots & C_p(O_q) & \ldots & C_p(O_n) \\ \vdots & \vdots & \ddots & \vdots & \ddots & \vdots \\ C_m & C_m(O_1) & \ldots & C_m(O_q) & \ldots & C_m(O_n) \end{array} \tag{1}$$

Let O denotes the set of all objects being evaluated, and $C(O)$ is the set of values assigned by a given criteria C (i.e., $C = C_p$ for some fixed p) to the objects, i.e.,

$$O \stackrel{\text{def}}{=} \{O_1, O_2, O_3, \ldots, O_n\}, \; C(O) \stackrel{\text{def}}{=} \{C(O_1), C(O_2), C(O_3), \ldots, C(O_n)\}.$$

Let $x_i = C(O_i)$. Then the following set can be defined:

$C^*(O) \stackrel{\text{def}}{=} \{\langle x_i, x_j\rangle | i \neq j \,\&\, \langle x_i, x_j\rangle \in C(O) \times C(O)\}$.

Further, if $x = C(O_i)$ and $y = C(O_j)$, $x \prec y$ will be written iff $i < j$.

In order to find the agreement between two criteria, the vectors of all internal comparisons for each criterion are constructed, which elements fulfill one of the three relations R, $\overline{R}$ and $\tilde{R}$. The nature of the relations is chosen such that for a fixed criterion C and any ordered pair $\langle x, y\rangle \in C^*(O)$:

$$\langle x, y\rangle \in R \Leftrightarrow \langle y, x\rangle \in \overline{R}, \tag{2}$$

$$\langle x, y\rangle \in \tilde{R} \Leftrightarrow \langle x, y\rangle \notin (R \cup \overline{R}), \tag{3}$$

$$R \cup \overline{R} \cup \tilde{R} = C^*(O). \tag{4}$$

For example, if "R" is the relation "$<$", then $\overline{R}$ is the relation "$>$", and vice versa.

For the effective calculation of the vector of internal comparisons (denoted further by $V(C)$) only the subset of $C(O) \times C(O)$ needs to be considered, namely:

$C^{\prec}(O) \stackrel{\text{def}}{=} \{\langle x, y\rangle |\, x \prec y \,\&\, \langle x, y\rangle \in C(O) \times C(O)$,

due to Eqs. (2)-(4). For brevity, $c^{i,j} = \langle C(O_i), C(O_j)\rangle$.

Then for a fixed criterion C the vector of lexicographically ordered pair elements is constructed:

$$V(C) = \{c^{1,2}, c^{1,3}, \ldots, c^{1,n}, c^{2,3}, c^{2,4}, \ldots, c^{2,n}, c^{3,4}, \ldots, c^{3,n}, \ldots, c^{n-1,n}\}. \tag{5}$$

In order to be more suitable for calculations, $V(C)$ is replaced by $\hat{V}(C)$, where its k-th component ($1 \leq k \leq \frac{n(n-1)}{2}$) is given by:

$$\hat{V_k}(C) = \begin{cases} 1, \text{ iff } V_k(C) \in R, \\ -1, \text{ iff } V_k(C) \in \overline{R}, \\ 0, \text{ otherwise.} \end{cases}$$

When comparing two criteria the degree of "agreement" ($\mu_{C,C'}$) is usually determined as the number of matching components of the respective vectors. The degree of "disagreement" ($\nu_{C,C'}$) is usually the number of components of opposing signs in the two vectors. From the way of computation it is obvious that $\mu_{C,C'} = \mu_{C',C}$ and $\nu_{C,C'} = \nu_{C',C}$. Moreover, $\langle \mu_{C,C'}, \nu_{C,C'}\rangle$ is an Intuitionistic Fuzzy Pair (IFP).

There may be some pairs $\langle \mu_{C,C'}, \nu_{C,C'}\rangle$, for which the sum $\mu_{C,C'} + \nu_{C,C'}$ is less than 1. The difference $\pi_{C,C'}$ is considered as a degree of "uncertainty:

$$\pi_{C,C'} = 1 - \mu_{C,C'} - \nu_{C,C'}. \tag{6}$$

In [37] five different algorithms for calculation of $\mu_{C,C'}$ and $\nu_{C,C'}$ are presented:

- **μ-biased ICrA algorithm**: This algorithm follows the rules presented in [13, Table 3], where the rule for $=,=$ for two criteria C and C' is assigned to $\mu_{C,C'}$.

- **ν-biased ICrA algorithm**: In this case the rule for $=,=$ for two criteria C and C' is assigned to $\nu_{C,C'}$. It should be noted that in such case a criteria compared to itself does not necessarily yield $\langle 1,0\rangle$.
- **Balanced ICrA algorithm**: This algorithm follows the rules in [13, Table 2], where the rule for $=,=$ for two criteria C and C' is assigned a half to both $\mu_{C,C'}$ and $\nu_{C,C'}$. It should be noted that in such case a criteria compared to itself does not necessarily yield $\langle 1,0\rangle$.
- **Unbiased ICrA algorithm**: This algorithm follows the rules in [13, Table 1]. It should be noted that in such case a criterion compared to itself does not necessarily yield $\langle 1,0\rangle$, too.
- **Weighted ICrA algorithm**: This algorithm is newly proposed and it is based on the Unbiased for the initial estimation of $\mu_{C,C'}$ and $\nu_{C,C'}$, however, at the end of it the values of $\pi_{C,C'}$ are proportionally distributed to $\mu_{C,C'}$ and $\nu_{C,C'}$. Thus, the final values of $\mu_{C,C'}$ and $\nu_{C,C'}$ generated by this algorithm will always complement to 1.

In this research μ-biased ICrA algorithm is applied. The pseudo-code of the algorithm is presented below as **Algorithm 1**.

Algorithm 1 : μ-biased

Require: Vectors $\hat{V}(C)$ and $\hat{V}(C')$

function DEGREES OF AGREEMENT AND DISAGREEMENT($\hat{V}(C),\hat{V}(C')$)
  $V \leftarrow \hat{V}(C)-\hat{V}(C')$
  $\mu \leftarrow 0$
  $\nu \leftarrow 0$
  for $i \leftarrow 1$ to $\frac{n(n-1)}{2}$ **do**
    if $V_i = 0$ **then**
      $\mu \leftarrow \mu + 1$
    else if $\text{abs}(V_i) = 2$ **then** ▷ $\text{abs}(V_i)$: the absolute value of V_i
      $\nu \leftarrow \nu + 1$
    end if
  end for
  $\mu \leftarrow \frac{2}{n(n-1)}\mu$
  $\nu \leftarrow \frac{2}{n(n-1)}\nu$
  return μ,ν
end function

As a result of applying ICrA to IM A (Eq. (1)), the following IM is constructed:

$$\begin{array}{c|ccc} & C_2 & \dots & C_m \\ \hline C_1 & \langle \mu_{C_1,C_2}, \nu_{C_1,C_2}\rangle & \dots & \langle \mu_{C_1,C_m}, \nu_{C_1,C_m}\rangle \\ \vdots & \vdots & \ddots & \vdots \\ C_{m-1} & \langle \mu_{C_{m-1},C_2}, \nu_{C_{m-1},C_2}\rangle & \dots & \langle \mu_{C_{m-1},C_m}, \nu_{C_{m-1},C_m}\rangle \end{array},$$

that determines the degrees of "agreement" (μ_{C_i,C_j}) and "disagreement" (ν_{C_i,C_j}) between criteria $C_1,...,C_m$ [9].

The analysis was carried out using the cross-platform software ICrAData [25]. The obtained ICrA results are analyzed based on the proposed in [13] consonance and dissonance scale. For ease of use the scheme for defining the consonance and dissonance between each pair of criteria is presented in Table 1.

Table 1. Consonance and dissonance scale [13]

Interval of $\mu_{C,C'}$	**Meaning**
[0.00-0.05]	strong negative consonance (SNC)
(0.05-0.15]	negative consonance (NC)
(0.15-0.25]	weak negative consonance (WNC)
(0.25-0.33]	weak dissonance (WD)
(0.33-0.43]	dissonance (D)
(0.43-0.57]	strong dissonance (SD)
(0.57-0.67]	dissonance (D)
(0.67-0.75]	weak dissonance (WD)
(0.75-0.85]	weak positive consonance (WPC)
(0.85-0.95]	positive consonance (PC)
(0.95-1.00]	strong positive consonance (SPC)

Chaos theory

Chaos is defined as a phenomenon to study the random and unpredictable deterministic behavior of the system. Chaos randomness is significantly distinct from statistical randomness in the context of inherent ability for search space in order to improve optimization. The following different types of chaotic maps (M1-M10) are used in the paper:

M1. Chebyshev map

According to [42, 43] the Chebyshev map is given by:

$$w_{n+1} = \cos(t\cos^{-1}(w_n)). \tag{7}$$

M2. Circle map

The following expression represents the circle map [29]:

$$w_{n+1} = w_n + \beta - (\alpha - 2\pi) \mod (1), \tag{8}$$

where $\alpha = 0.5, \beta = 0.2$.

M3. Gauss map

The nonlinear Gauss map (also known as mouse map, [29]) can be expressed as:

$$w_{n+1} = \exp(-\alpha w_n^2) + \beta, \tag{9}$$

where α and β are real parameters.

M4. Iterative map

This chaotic map is defined by [32]:

$$w_{n+1} = \sin\left(\frac{\alpha\pi}{w_n}\right), \tag{10}$$

where $\alpha \in (0,\ 1)$.

M5. Logistic map

A logistic map explains the complex behavior without the randomness appeared from deterministic system which is defined as follows [31]:

$$w_{n+1} = cw_n(1 - w_n), \tag{11}$$

where $w_0 \in (0,\ 1)$, $w_0 \notin \{0,\ 0.25,\ 0.50,\ 0.75,\ 1\}$, $c = 4$ is called a chaotic sequence.

M6. Piecewise map

The piecewise map [32] is defined as follows:

$$w_{n+1} = \begin{cases} \dfrac{w_n}{k}, & 0 < w_n < k \\ \dfrac{w_n - k}{0.5 - k}, & k \leq w_n < 0.5 \\ \dfrac{1 - k - w_n}{0.5 - k}, & 0.5 \leq w_n < 1 - k \\ \dfrac{1 - w_n}{k}, & 1 - k < w_n < 1 \end{cases} \tag{12}$$

M7. Sine map

The mathematical formulation of sine map [23] is:

$$w_{n+1} = \frac{\alpha}{4}(\sin \pi w_n), \tag{13}$$

where $0 < \alpha \leq 4$.

M8. Singer map

Singer map can be expressed as [15]:

$$w_{n+1} = \mu(7.86w_n - 23.31w_n^2 + 28.75w_n^3 - 13.302875w_n^4), \tag{14}$$

where $\mu \in (0.9,\ 1.08)$.

M9. Sinusoidal map

Mathematically, the sinusoidal map can be expressed as [31]:

$$w_{n+1} = \alpha w_t^2 \sin(\pi w_n), \tag{15}$$

where $\alpha = 2.3$.

M10. Tent map

Tent map is expressed by the following equation [33]:

$$w_{n+1} = \begin{cases} \dfrac{w_n}{0.07}, & w_n < 0.7 \\ \dfrac{10(1-w_n)}{3}, & w_n \geq 0.7 \end{cases} \tag{16}$$

The advantages of chaos theory with non-invertible map scan carry out the overall search space at a higher speed than stochastic search [26, 27] due to the non-repetition and ergodicity of chaos [28]. It depends on searching of global optimum on chaotic motion properties such as ergodicity, regularity and stochastic properties.

Electromagnetic field optimization

EFO is a population-based algorithm and each solution vector is represented by one group of electromagnets (electromagnetic particle). In essence, EFO leverages the principles of electromagnetism to guide the search for optimal solutions. The interplay of attractive and rotational forces allows the algorithm to effectively explore the solution space and converge towards promising regions. The number of electromagnets of an electromagnetic particle is determined by the number of variables of the optimization problem. Therefore, each electromagnet of the electromagnetic particle corresponds to one variable of the optimization problem. Moreover, all electromagnets of the same electromagnetic particle have the same polarity. However, each electromagnet can apply a force of attraction or repulsion on the peer-electromagnets that correspond to the same variable of the optimization problem.

According to [1], the EFO works as follows:

- First, a population of electromagnetic particles is generated randomly, and the fitness of each particle is evaluated by a fitness function; then, particles are sorted according to their fitness.
- Second, sorted particles are divided into three groups, and a portion of the electromagnetic population is allocated to each group; the first group is called the positive field and consists of the fittest electromagnetic particles with positive polarity, the second group is called the the negative field and consists of the electromagnetic particles with the lowest fitness and negative polarity, and the remaining electromagnetic particles form a group called the neutral field, which has a small negative polarity almost near zero.
- Finally, in each iteration of the algorithm, a new electromagnetic particle is shaped and evaluated by a fitness function. If the generated electromagnetic particle is fitter than the worst electromagnetic particle in the population, then the generated particle will be inserted into the sorted population according to its fitness and obtain a polarity based on its position in the population; moreover, the worst particle will be eliminated.

This process continues until it reaches the maximum number of iterations or finds the expected near-optimal solution.

EFO determines the position of each electromagnet of a generated electromagnetic particle as follows: from the electromagnetic particles of each electromagnetic field (positive, negative,

and neutral), three peer electromagnets are randomly selected (one electromagnet from each field). Afterwards, the generated electromagnet gets the position and polarity (small negative polarity) of the selected electromagnet from the neutral field and gets affected by the selected electromagnets from the positive field (attraction) and negative field (repulsion) by random force intensity. In other words, the generated electromagnet moves a distance away from the bad solutions and approaches good solutions [1].

The coexistence of two opposite forces among electromagnets and the fact that the new solution is generated by moving a distance away from bad solutions and moving closer to the good solutions cause effective search and fast convergence. However, to keep diversity and avoid local minima, randomness is an indispensable part of EFO. Therefore, for some of the generated electromagnetic particles (not all), only one of the electromagnets is changed with a randomly generated electromagnet. The reason for applying randomness to some electromagnetic particles is that the existence of the random variables in all solutions will prevent finding a good solution. However, applying randomness to some solutions brings diversity into the population and prevents local minima [1].

EFO parameters setting plays a significant role in the performance of EFO. The most important parameter of EFO is N_{emp}, which determines the number of electromagnetic particles of the population. A small number of particles inside the population will cause finding local minima instead of global minima due to the lack of knowledge about the search space. Additionally, a large population will lead to slow convergence. In [1] is found out that a population smaller than 50 tends to find local minima, and a population greater than problem dimension increases the computational time.

The parameters P_{field} and N_{field} parameters determine the percentage of the allocated population to the each of the three groups with different polarities. Other important parameters of EFO are Ps_{rate} (the probability of selecting electromagnets of the generated electromagnetic particle from electromagnets of the positive field without changing them) and R_{rate} (the possibility of changing one electromagnet of the generated electromagnetic particle with a randomly generated electromagnet). In Table 2 the proposed in [1] range of parameters values are presented.

Table 2. Range of the main EFO parameters

Parameters	**Value**
P_{field}	0.05 - 0.1
N_{field}	0.4 - 0.5
Ps_{rate}	0.1 - 0.4
R_{rate}	0.1 - 0.4

A large value for P_{field} increases the global search and slows down convergence, while a small value for P_{field} reduces the global search and increases the local search [1]. Here, Eq. (17) is used for calculation of the N_{field} value:

$$N_{field} = \frac{1 - P_{field}}{2}. \tag{17}$$

Based on a set of numerical experiments other EFO parameters are set to the following values:

$N_{emp} = 50$;
$P_{field} = 0.1$;
$N_{field} = 0.45$;
$Ps_{rate} = 0.2$;
$R_{rate} = 0.4$; and
$Max_{gen} = 200$ (maximum number of iterations).

EFO offers several key advantages as an optimization algorithm:

1. Exploration and Exploitation Balance: EFO effectively balances exploration of the solution space with exploitation of promising regions.
    - The electric force drives particles towards areas of higher fitness (better solutions), encouraging exploitation.
    - The magnetic force introduces a rotational component, forcing particles to explore different directions and preventing them from getting stuck in local optima.
2. Versatility: EFO can be applied to a wide range of optimization problems, including:
    - Continuous optimization problems
    - Discrete optimization problems
    - Constrained optimization problems
3. Simplicity: The core concept of EFO is relatively easy to understand and implement.
4. Efficiency: In many cases, EFO can efficiently find high-quality solutions, especially for complex optimization problems.
5. Robustness: EFO has shown robustness in handling various types of optimization landscapes and can often avoid getting trapped in local optima.

These advantages make EFO a valuable tool for solving challenging optimization problems across diverse domains, including engineering, machine learning, and finance.

Case study

As a case study the model parameter identification problem of a non-linear fed-batch cultivation process of *E. coli* BL21(DE3)pPhyt109 is used. The following differential equation system is considered [16, 36]:

$$\frac{dX}{dt} = \mu X - \frac{F_{in}}{V} X, \tag{18}$$

$$\frac{dS}{dt} = -q_S X + \frac{F_{in}}{V}(S_{in} - S), \tag{19}$$

$$\frac{dP}{dt} = q_P X - \frac{F_{in}}{V} P, \tag{20}$$

$$\frac{dV}{dt} = F_{in}, \tag{21}$$

where

$$\mu = \mu_{max}\frac{S}{k_S + S},$$
$$q_S = \frac{1}{Y_{S/X}}\mu, \tag{22}$$
$$q_P = \frac{1}{Y_{P/X}}\mu,$$

and X is the biomass concentration, [g/l]; S is the substrate concentration, [g/l]; P is the product concentration, [g/l]; F_{in} is the feeding rate, [l/h]; V is the bioreactor volume, [l]; S_{in} is the substrate concentration in the feeding solution, [g/l]; μ, q_S and q_P are the specific rate functions, [1/h]; μ_{max} is the maximum specific growth rate, [1/h]; k_S is the saturation constant, [g/l]; $Y_{S/X}$ and $Y_{P/X}$ are the yield coefficients, [-].

For the model (Eqs. (18)-(22)) the parameters that will be identified are:

μ_{max}, k_S, $Y_{S/X}$ and $Y_{P/X}$.

Let
$Z_{\text{mod}} \stackrel{\text{def}}{=} [X_{\text{mod}}\ S_{\text{mod}}\ P_{\text{mod}}]$ (model predictions for biomass and substrate) and
$Z_{\text{exp}} \stackrel{\text{def}}{=} [X_{\text{exp}}\ S_{\text{exp}}\ P_{\text{exp}}]$ (known experimental data for biomass and substrate).

Then putting $Z = Z_{\text{mod}} - Z_{\text{exp}}$, we define the objective function as:

$$J = \|Z\|^2 \to \min, \tag{23}$$

where $\|\|$ denotes the ℓ^2-vector norm.

For the model parameters identification we use experimental data for biomass, glucose and product concentrations of an *E. coli* BL21(DE3)pPhyt109 fed-batch cultivation process. The detailed description of the process condition and experimental data are presented in [35].

Results and discussion

Numerical results

The proposed mathematical model consists of a set of four ODEs (Eqs.18-21) with three dependent state variables $x = [X\ S\ P]$ and four unknown parameters $p = [\mu_{max}\ k_S\ Y_{S/X}\ Y_{P/X}]$.

The ranges of the model parameters are as follows:

$$\begin{aligned} &0.1 \le \mu_{max} \le 0.9;\\ &0.001 \le k_S \le 0.5;\\ &0.5 \le Y_{S/X} \le 10;\\ &0.5 \le Y_{P/X} \le 10. \end{aligned} \tag{24}$$

The numerical experiments were performed on Intel® Core™i7-8700 CPU @ 3.20 GHz, 3192 MHz, 32 GB Memory (RAM), with a Windows 10 pro (64 bit) operating system. The considered competing algorithms were implemented in Matlab R2019a. The mathematical model of

E. coli was created in the Simulink R2019a environment. The solver options were the automatic variable step size and ode45 (Runge–Kutta).

Series of 30 runs of each EFO algorithm are performed on the test case – cultivation model parameters identification problem. The model parameters are estimated by 10 different EFO algorithms using different chaotic maps, as follows: EFO algorithm M1 using Chebyshev chaotic map, M2 – Circle chaotic map, M3 – Gauss chaotic map, M4 – Iterative chaotic map, M5 – Logistic chaotic map, M6 – Piecewise chaotic map, M7 – Sine chaotic map, M8 – Singer chaotic map, M9 – Sinusoidal chaotic map, and M10 – Tent chaotic map. Due to the stochastic nature of the applied algorithms series of 30 runs for each algorithm are performed. The obtained best estimates of the model parameters, as well as the corresponding value of objective function J are presented in Table 3. The best three results are marked in bold.

Table 3. Optimization results

Algorithm chaotic map	**Objective function value**	μ_{max}	k_S	$Y_{S/X}$	$Y_{P/X}$
M1	123.646	0.85	0.016	2.29	1.93
M2	122.805	0.71	0.004	2.27	1.98
M3	**121.533**	0.85	0.013	2.27	1.95
M4	**121.546**	0.78	0.008	2.28	1.96
M5	121.744	0.77	0.005	2.29	1.98
M6	122.688	0.87	0.015	2.21	1.89
M7	121.732	0.85	0.009	2.24	1.93
M8	123.155	0.82	0.008	2.32	2.02
M9	**121.308**	0.85	0.006	2.28	1.97
M10	122.294	0.88	0.016	2.30	1.99

As can be seen, the best objective function values are obtained based on EFO algorithm with Gauss, Iterative and Sinusoidal chaotic maps. The worst results are observed for EFO with Chebyshev and Singer chaotic maps. The performance of EFO with Logistic and Sine chaotic maps is identical, as well as the performance of Circle and Piecewise chaotic maps.

A graphical comparisons can be used to establish the presence or absence of systematic deviations between the model predictions and the real measurements (experimental data). Such quantitative measure is also an important evidence for the adequacy of the obtained models. The model predictions of the state variables X, S and P, based on 10 estimated sets of model parameters, are compared to the experimental data of *E. coli* fed-batch process in Figs. 1-3.

The graphical results show that the all models fit well the experimental data. Only model M2 (Circle chaotic map) show some different behaviour for the substrate dynamics.

To compare the performance of the 10 considered EFO algorithms statistical analysis of the numerical results are performed. The data from 30 runs of the algorithms, e.g., the observed values of the objective function J and the estimated values of the model parameters (μ_{max}, k_S, $Y_{S/X}$ and $Y_{P/X}$), are analysed. The summary statistics of the results (mean values, SD, and the median

of the estimated values) are presented as box plot diagrams in Fig. 4, Fig. 5 and Fig. 6.

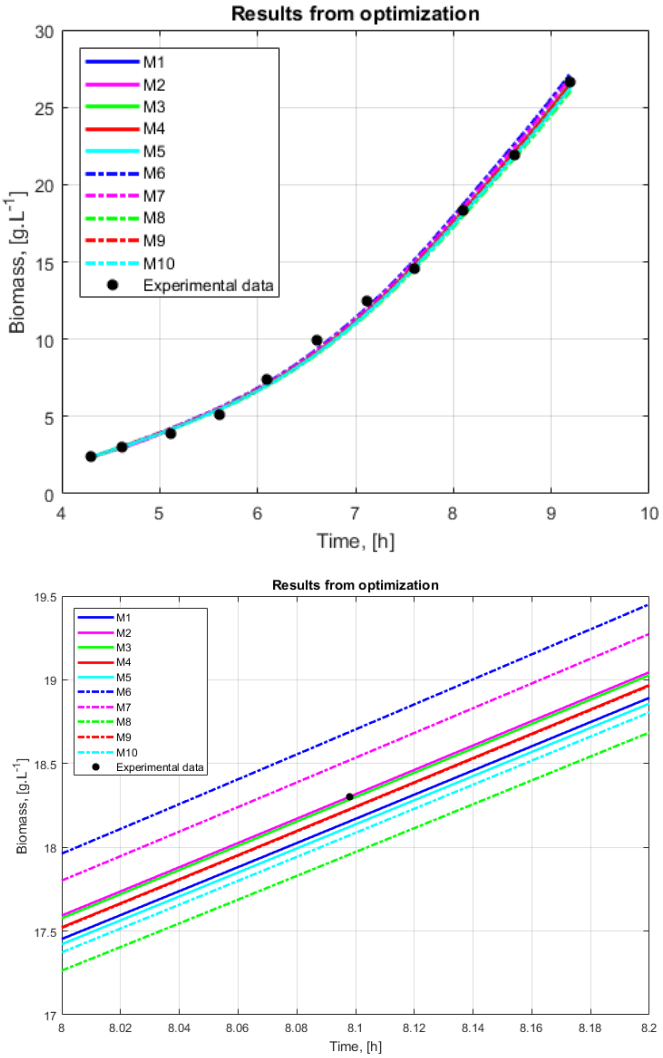

Fig. 1 Experimental data and models predictions for biomass concentration of an *E. coli* BL21(DE3)pPhyt109 cultivation model

The results show that the best J value observed for M3 is an outlier value. The best mean result for J is achieved by M4. Given the data for J values, the algorithms M1, M2, M3, M8 and M9 do not produce results with a normal distribution. In the case of model parameters value data, only a few EFO algorithms show a normal distribution of the estimates. The considered model parameter identification problem is very complex. The mathematical model is highly non-linear and the use of row experimental data makes the problem difficult to solve. This is why all EFO algorithms exhibit such behaviour – the longer the box, the more dispersed the data and the data distribution is positive or negative skewed (Figs. 5 and 6).

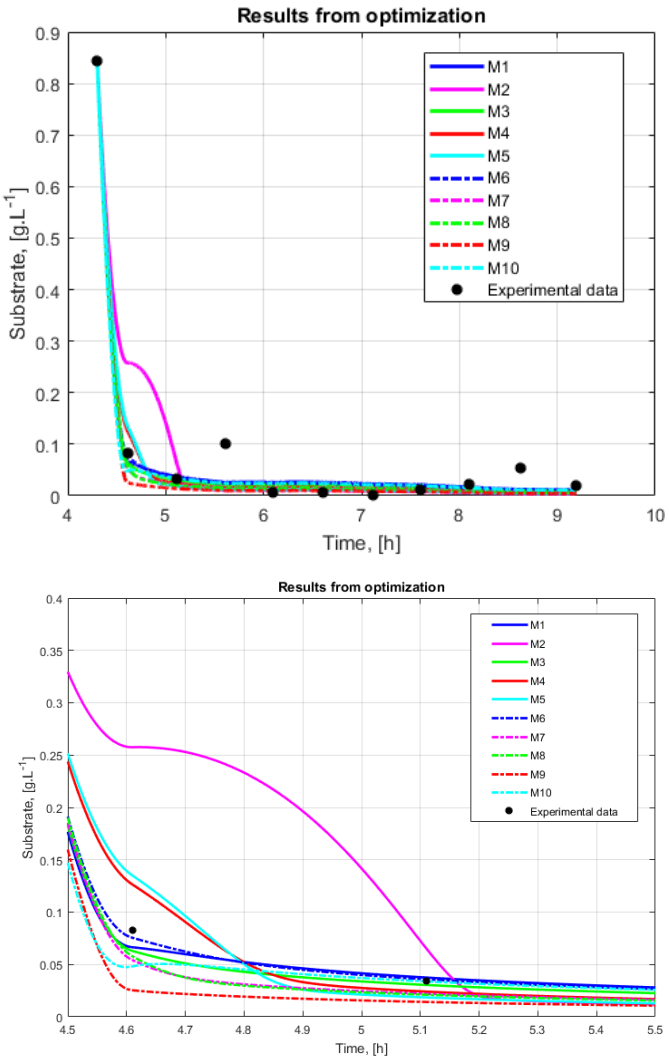

Fig. 2 Experimental data and models predictions for substrate concentration of an *E. coli* BL21(DE3)pPhyt109 cultivation model

Based on the numerical results (obtained objective function values) the algorithms M9, M4 and M3 find solutions with the higher accuracy. However, the statistical analysis show that the M3 and M9 do not have good distribution of the estimates. So, the EFO algorithm M4, using Iterative chaotic map, is the algorithm with the best overall performance.

Application of ICrA

To perform ICrA ten IMs are constructed. Each IM consists 30 columns (30 runs of EFO algorithms) and 5 rows (results for J and four model parameters) as follows:

$$Input\ IM_i = \begin{array}{c|cccc} & Run1 & Run2 & \dots & Run30 \\ \hline J & & & \dots & \\ \mu_{max} & & & \dots & \\ k_S & & & \dots & \\ Y_{S/X} & & & \dots & \\ Y_{P/X} & & & \dots & \end{array},$$

where the obtained estimations for J and model parameters are used; $i = 1 \div 10$, for M1 to M10.

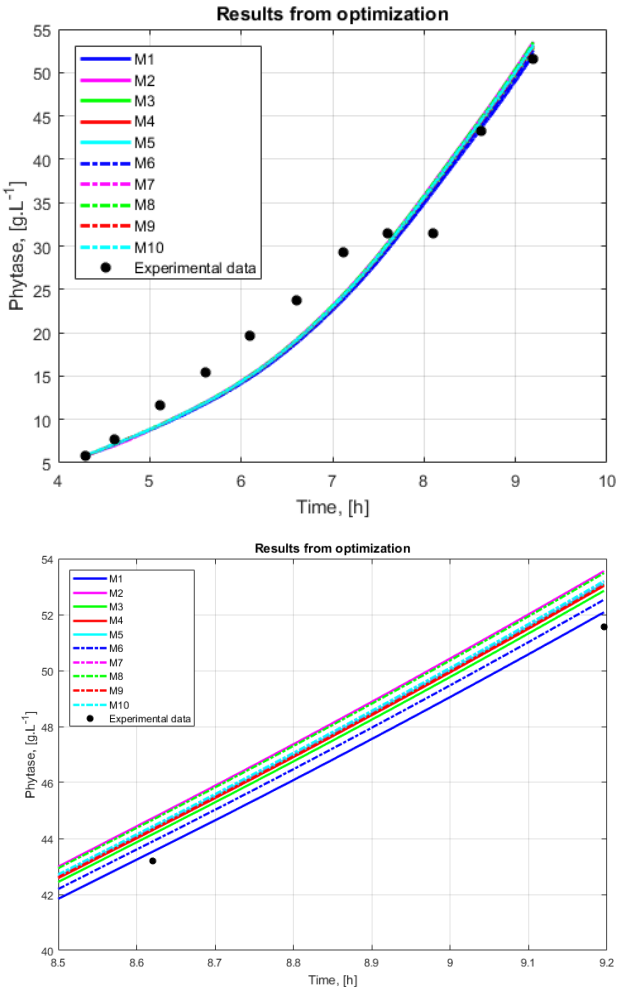

Fig. 3 Experimental data and models predictions for product concentration of an *E. coli* BL21(DE3)pPhyt109 cultivation model

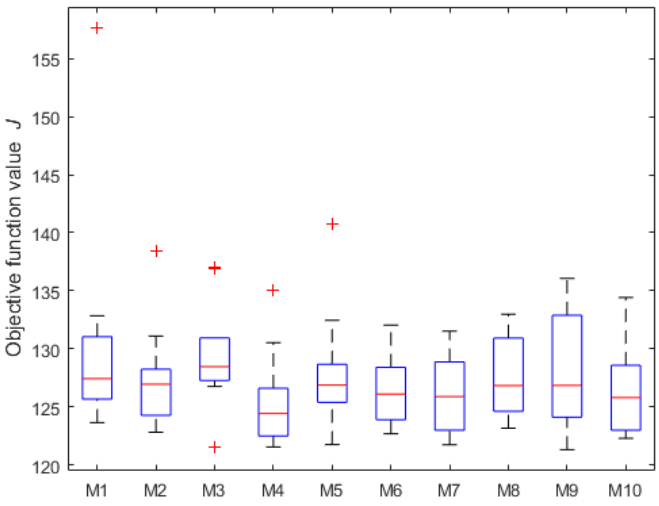

Fig. 4 Box plot with the results from the parameter identification – objective function value

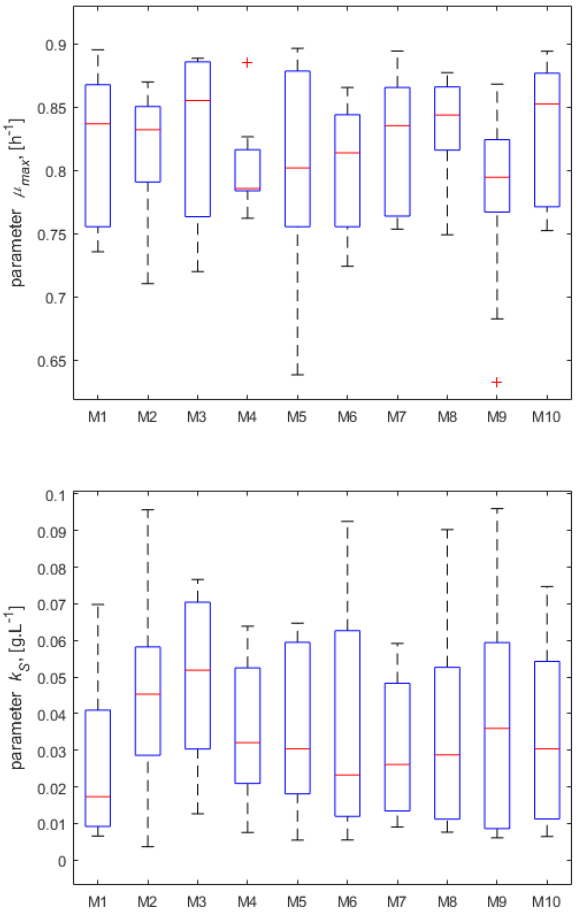

Fig. 5 Box plot with the results from the parameter identification – model parameters μ_{max} and k_S

In the beginning, the ICrA is applied to the 10 IM_i. As a result the following IMs are obtained:

$Output_1\ IM_i =$

	J	μ_{max}	k_S	$Y_{S/X}$	$Y_{P/X}$
J	1	$\langle \mu_{J,\mu_{max}}, \nu_{J,\mu_{max}} \rangle$	...	...	$\langle \mu_{J,Y_{P/X}}, \nu_{J,Y_{P/X}} \rangle$
μ_{max}	$\langle \mu_{\mu_{max},J}, \nu_{\mu_{max},J} \rangle$	1	...	...	$\langle \mu_{\mu_{max},Y_{P/X}}, \nu_{\mu_{max},Y_{P/X}} \rangle$,
$\vdots$	$\vdots$	$\vdots$	$\vdots$	$\vdots$	$\vdots$
$Y_{P/X}$	$\langle \mu_{Y_{P/X},J}, \nu_{Y_{P/X},J} \rangle$	$\langle \mu_{Y_{P/X},\mu_{max}}, \nu_{Y_{P/X},\mu_{max}} \rangle$	...	...	1

To evaluate the correlations between the 10 EFO (M1-M10) the ICrA is again performed over the IMs $Output_1 IM_i$. Thus, the considered ICrA criteria C are the 10 EFO algorithms – M1 is $C1$, M2 is $C2$, etc. As a result an IM of the correlations between criteria C_i is obtained.

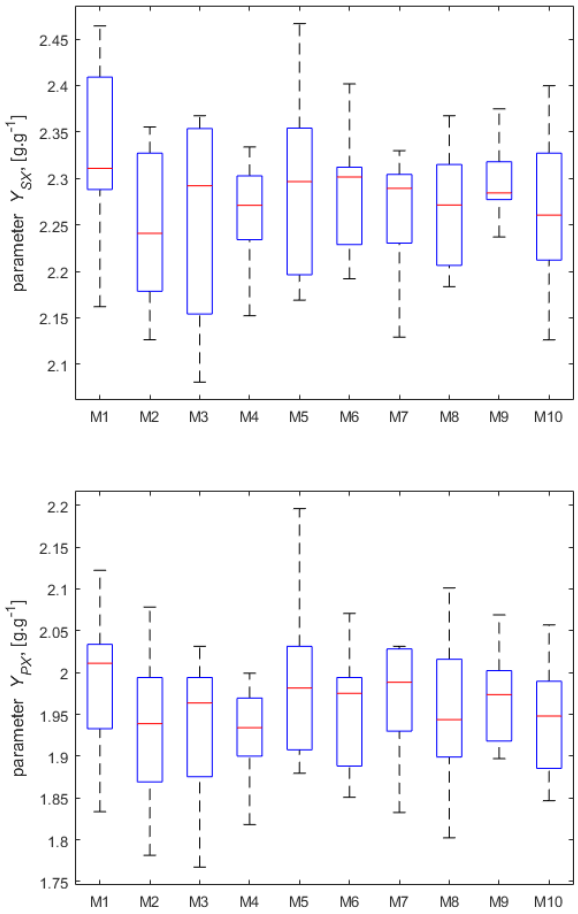

Fig. 6 Box plot with the results from the parameter identification: model parameters $Y_{S/X}$ and $Y_{P/X}$

The resulting degree of "agreement" (μ_{C_i,C_j}) and "disagreement" (ν_{C_i,C_j}) between the criteria are presented as IMs, as follows:

$Output_2\ IM_{\mu_{C_i,C_j}} =$

	M1	M2	M3	M4	M5	M6	M7	M8	M9	M10
M1	1.00	0.36	0.44	0.51	**0.78**	0.47	0.42	0.58	0.49	0.56
M2	0.36	1.00	0.60	0.71	0.56	**0.78**	**0.82**	0.53	0.71	0.60
M3	0.44	0.60	1.00	0.67	0.38	0.51	0.51	0.40	0.42	0.58
M4	0.51	0.71	0.67	1.00	0.56	0.58	0.60	0.69	0.53	**0.89**
M5	**0.78**	0.56	0.38	0.56	1.00	0.60	0.60	0.53	0.64	0.51
M6	0.47	**0.78**	0.51	0.58	0.60	1.00	**0.89**	0.51	**0.82**	0.51
M7	0.42	**0.82**	0.51	0.60	0.60	**0.89**	1.00	0.53	**0.84**	0.51
M8	0.58	0.53	0.40	0.69	0.53	0.51	0.53	1.00	0.53	**0.76**
M9	0.49	0.71	0.42	0.53	0.64	**0.82**	**0.84**	0.53	1.00	0.49
M10	0.56	0.60	0.58	**0.89**	0.51	0.51	0.51	**0.76**	0.49	1.00

$Output_2\ IM_{v_{C_i,C_j}}$ =

	M1	M2	M3	M4	M5	M6	M7	M8	M9	M10
M1	0.00	0.58	0.49	0.47	0.13	0.44	0.53	0.38	0.44	0.38
M2	0.58	0.00	0.31	0.24	0.42	0.11	0.11	0.40	0.20	0.31
M3	0.49	0.31	0.00	0.29	0.51	0.38	0.42	0.53	0.49	0.33
M4	0.47	0.24	0.29	0.00	0.38	0.36	0.38	0.29	0.42	0.07
M5	0.13	0.42	0.51	0.38	0.00	0.27	0.36	0.38	0.24	0.38
M6	0.44	0.11	0.38	0.36	0.27	0.00	0.02	0.40	0.07	0.38
M7	0.53	0.11	0.42	0.38	0.36	0.02	0.00	0.42	0.09	0.42
M8	0.38	0.40	0.53	0.29	0.38	0.40	0.42	0.00	0.40	0.18
M9	0.44	0.20	0.49	0.42	0.24	0.07	0.09	0.40	0.00	0.42
M10	0.38	0.31	0.33	0.07	0.38	0.38	0.42	0.18	0.42	0.00

The obtained results are visualized in Fig. 7.

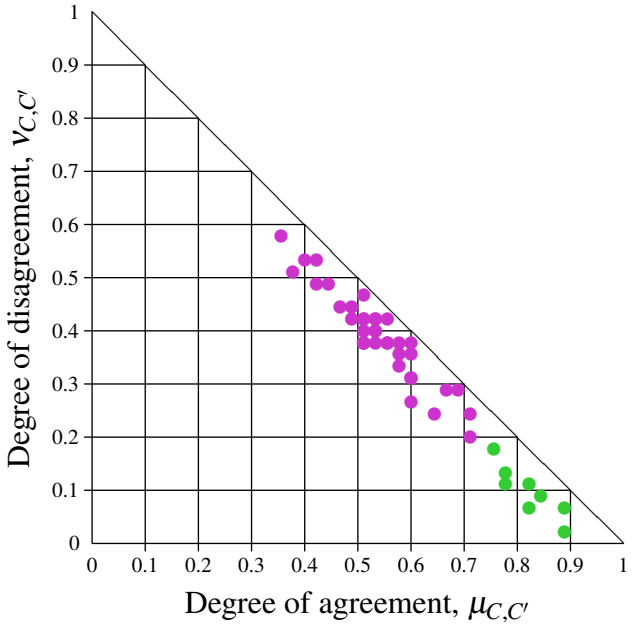

Fig. 7 Representation of the results in the intuitionistic fuzzy interpretation triangle

The EFO algorithms that show similar performance, based on the ICrA results, are the following (in descending order of similarity):

Group 1 M4-M10, M6-M7;

Group 2 M7-M9, M2-M7, M6-M9;

Group 3 M1-M5, M2-M6, M8-M10.

It is found that EFO algorithms M6 (Piecewise chaotic map) and M7 (Sine chaotic map) have similar performance. These algorithms are related with the algorithms M2 (Circle chaotic map)

and M9 (Sinusoidal chaotic map). Only EFO algorithm M3 (Gauss chaotic map) show performance that is not related to the performance of the other 9 EFO algorithms. The higher degree of agreement is found for the M4-M10. M4 (Iterative chaotic map) is the best performed EFO algorithm and M10 (Tent chaotic map) is one of the algorithms that produces best mean J value.

The conducted analyses, both statistical and ICrA, made it possible to determine the best among the ten EFO algorithms. M4 and M10 are selected as the algorithms with the best performance.

Conclusion

The performance of 10 different EFO algorithms is investigated. As a case study, *E. coli* BL21(DE3)pPhyt109, a non-linear fed-batch cultivation process is used. Different chaotic maps are incorporated in each EFO. The results obtained using Chebyshev, Circle, Gaussian, Iterative, Logistic, Partial, Sinusoidal, Singer, Sinusoidal and Tent chaotic maps are compared. Based on the performed statistical analysis and InterCriteria analysis, EFO with Iterative chaotic map and EFO with Tent chaotic map are indicated as the best performed EFO algorithms.

As future work directions, the results obtained here can be confirmed (i) based on the application of the chaotic EFO algorithms to another case study, or (ii) the same chaotic maps be incorporated in another metaheuristic algorithm applied to the model parameter identification of an *E. coli* BL21(DE3)pPhyt109 non-linear fed-batch cultivation process.

Acknowledgements

DZ thanks the National Science Fund of Bulgaria under Grant No. KN-06-N-22/1 "Theoretical Research and Applications of InterCriteria Analysis" for its support.

References

1. Abedinpourshotorban H., S. M. Shamsuddin, Z. Beheshti, D. N.A. Jawawi (2016). Electromagnetic Field Optimization: A Physics-inspired Metaheuristic Optimization Algorithm, Swarm and Evolutionary Computation, 26, 8-22.
2. Ahmad S. (2022). Electromagnetic Field Optimization Based Selective Harmonic Elimination in a Cascaded Symmetric H-bridge Inverter, Energies, 15(20), 7682.
3. Akbarzadeh M. R., H. Ghafourian, A. Anvari, R. Pourhanasa, et al. (2023). Estimating Compressive Strength of Concrete Using Neural Electromagnetic Field Optimization, Materials, 16(11), 4200.
4. Akpamukcu M., A. Ates, O. Akdag (2023). Combination of Electromagnetic Field and Harris Hawks Optimization Algorithms with Optimization to Optimization Structure and Its Application for Optimum Power Flow, Journal of the Chinese Institute of Engineers, 46(7), 754-765.
5. Aranguren I., A. Valdivia, M. Pérez-Cisneros, D. Oliva,et al. (2022). Digital Image Thresholding by Using a Lateral Inhibition 2D Histogram and a Mutated Electromagnetic Field Optimization, Multimedia Tools and Applications, 81(7), 10023-10049.
6. Atanassov K. (2012). On Intuitionistic Fuzzy Sets Theory, Springer, Berlin.
7. Atanassov K. (2014). Index Matrices: Towards an Augmented Matrix Calculus, Studies in Computational Intelligence, 573.
8. Atanassov K. (2016). Intuitionistic Fuzzy Sets, VII ITKR Session, Sofia, 20-23 June 1983, Reprinted: International Journal Bioautomation, 20(S1), S1-S6.
9. Atanassov K., D. Mavrov, V. Atanassova (2014). InterCriteria Decision Making: A New Approach for Multicriteria Decision Making, Based on Index Matrices and Intuitionistic Fuzzy Sets, Issues in Intuitionistic Fuzzy Sets and Generalized Nets, 11, 1-8.
10. Atanassov K. (2010). On Index Matrices, Part 1: Standard Cases, Advanced Studies in Contemporary Mathematics, 20(2), 291-302.

11. Atanassov K. (1987). Generalized Index Matrices, Comptes rendus de l'Academie Bulgare des Sciences, 40(11), 15-18.
12. Atanassov K. (2010). On Index Matrices, Part 2: Intuitionistic Fuzzy Case, Proceedings of the Jangjeon Mathematical Society, 13(2), 121-126.
13. Atanassov K., V. Atanassova, G. Gluhchev (2015). InterCriteria Analysis: Ideas and Problems, Notes on Intuitionistic Fuzzy Sets, 21(1), 81-88.
14. Atanassov K. (2016). Review and New Results on Intuitionistic Fuzzy Sets, Mathematical Foundations of Artificial Intelligence Seminar, Sofia, 1988, Preprint IM-MFAIS-1-88, Reprinted: Int J Bioautomation, 20(S1), S7-S16.
15. Barton R. (1990). Chaos and Fractals, Math Teach, 83(7), 524-529.
16. Bastin G., D. Dochain (1991). On-line Estimation and Adaptive Control of Bioreactors, Els. Sc. Publ.
17. Bouchekara H. (2020). Solution of the Optimal Power Flow Problem Considering Security Constraints Using an Improved Chaotic Electromagnetic Field Optimization Algorithm, Neural Comput & Applic, 32, 2683-2703.
18. Bureva V., S. Sotirov (2023). InterCriteria Analysis as an Intelligent Tool for Intuitionistic Fuzzy Decision Making: Case Study of Statistics for Science, Technology and Information Society of Turkish Statistical Institute, Proceeding of the International Conference on Intelligent and Fuzzy Systems, 525-531.
19. Chakraborty S., K. Mali (2020). Fuzzy Electromagnetism Optimization (Femo) and Its Application in Biomedical Image Segmentation, Appl Soft Comput, 97, 106800.
20. Chorukova E., P. Marinov, I. Umlenski (2021). Survey on Theory and Applications of InterCriteria Analysis Approach, Research in Computer Science in the Bulgarian Academy of Sciences, Studies in Computational Intelligence, 934, 453-469.
21. Coelho L. D. S., V. C. Mariani, S. K. Goudos, A. D. Boursianis, K. Kokkinidis, N. V. Kantartzis (2021). Chaotic Jaya Approaches to Solving Electromagnetic Optimization Benchmark Problems, Telecom, 2(2), 222-231.
22. Danailova-Veleva S., L. Doukovska, A. Dukovski (2022). InterCriteria Analysis of the Supervisory Statistic Data for Selected 8 EU Countries During the Period 2020-2021, Proceedings of the International Workshop on Intuitionistic Fuzzy Sets and Generalized Nets, 129-137.
23. Devaney R. (2008). An Introduction to Chaotic Dynamical Systems, Westview Press, Boulder.
24. Ibrahim A. M., M. A. Tawhid (2023). Chaotic Electromagnetic Field Optimization, Artif Intell Rev, 56, 9989–10030.
25. Ikonomov N. , P. Vassilev, O. Roeva (2018). ICrAData – Software for InterCriteria Analysis, Int J Bioautomation, 22(1), 1-10.
26. Erramilli A., R. Singh, P. Pruthi (1994a). Modeling Packet Traffic with Chaotic Maps, KTH, Stockholm.
27. Erramilli A., R. Singh, P. Pruthi (1994). Chaotic Maps as Models of Packet Traffic, Teletraffic Science and Engineering, Labetoulle J., J. W. Roberts (Eds.), Vol. 1, 329-338.
28. Eckmann J.-P., D. Ruelle (1985). Ergodic Theory of Chaos and Strange Attractors, Rev Mod Phys, 57(3), 617.
29. Hilborn R. C. (2000). Chaos and Nonlinear Dynamics: An Introduction for Scientists and Engineers, Oxford University Press on Demand, Oxford.
30. Kushwaha N., M. Pant, S. Sharma (2022). Electromagnetic Optimization-based Clustering Algorithm, Expert Systems, 39(7), e12491.
31. Li Y., S. Deng, D. Xiao (2011). A Novel Hash Algorithm Construction Based on Chaotic Neural Network, Neural Comput Appl, 20(1), 133-141.
32. May R. M. (1976). Simple Mathematical Models with Very Complicated Dynamics, Nature, 261(5560), 459-467.

33. Ott E. (2002). Chaos in Dynamical Systems, Cambridge University Press, Cambridge.
34. Ristić-Djurović J. L., S. S. Gajić, A. Ž. Ilić, N. Romčević, et al. (2017). Design and Optimization of Electromagnets for Biomedical Experiments with Static Magnetic and ELF Electromagnetic Fields, IEEE Transactions On Industrial Electronics, 65(6), 4991-5000.
35. Roeva O., T. Pencheva, B. Hitzmann, St. Tzonkov (2004). A Genetic Algorithms Based Approach for Identification of *Escherichia coli* Fed-batch Fermentation, Int. J. Bioautomation, 1, 30-41.
36. Roeva O. (2008). Improvement of Genetic Algorithm Performance for Identification of Cultivation Process Models, Advanced Topics on Evolutionary Computing, Book Series: Artificial Intelligence Series – WSEAS, 34-39.
37. Roeva O., P. Vassilev, N. Ikonomov, M. Angelova, et al. (2019). On Different Algorithms for InterCriteria Relations Calculation, Studies in Computational Intelligence, 757, 143-160.
38. Sartori C. A., A. Orlandi, G. Antonini (2000). Optimization of the LPS Configuration for Minimization of the Radiated Electromagnetic Field, Proceedings of the IEEE International Symposium on Electromagnetic Compatibility, Vol. 2, 827-832.
39. Song S., H. Jia, J. Ma (2019). A Chaotic Electromagnetic Field Optimization Algorithm Based on Fuzzy Entropy for Multilevel Thresholding Color Image Segmentation, Entropy, 21(4), 398.
40. Sultan H. M., A. S. Menesy, S. Kamel, R. A. Turky, et al. (2021). Optimal Values of Unknown Parameters of Polymer Electrolyte Membrane Fuel Cells Using Improved Chaotic Electromagnetic Field Optimization, IEEE Transactions on Industry Applications, 57(6), 6669-6687.
41. Talebi B., M. N. Dehkordi (2018). Sensitive Association Rules Hiding Using Electromagnetic Field Optimization Algorithm, Expert Systems with Applications, 114, 155-172.
42. Tavazoei M. S., M. Haeri (2007a). An Optimization Algorithm Based on Chaotic Behavior and Fractal Nature, J Comput Appl Math, 206(2), 1070-1081.
43. Tavazoei M. S., M. Haeri (2007b). Comparison of Different Onedimensional Maps as Chaotic Search Pattern in Chaos Optimization Algorithms, Appl Math Comput, 187(2), 1076-1085.
44. Todinova S., D. Mavrov, S. Krumova, P. Marinov, V. Atanassova, K. Atanassov, S. G. Taneva (2016). Blood Plasma Thermograms Dataset Analysisby Means of InterCriteria and Correlation Analyses for the Case of Colorectal Cancer, Int J Bioautomation, 20(1), 115-124.
45. Traneva V., S. Tranev (2023). Multi-layered InterCriteria Analysis as a Digital Tool for Studying the Dependencies of Some Key Indicators of Mortality During the Pandemic in the European Union, Intelligent Systems in Digital Transformation: Theory and Applications, 267-293.
46. Vassilev V., H. Hlebarov, S. Ribagin, K. Atanassov (2022) InterCriteria Analysis of Data Obtained from Patients with Hypercholesterolemia Treated with Linoprixol, Proceedings of the International Symposium on Bioinformatics and Biomedicine, 65-71.
47. Viesturs U., D. Karklina, I. Ciprovica (2004). Bioprocess and Bioengineering, Jeglava.
48. Yanan D. U., G. Hongyuan, C. H. E. N. Menghan (2021). Direction of Arrival Estimation Method Based on Quantum Electromagnetic Field Optimization in the Impulse Noise, Journal of Systems Engineering and Electronics, 32(3), 527-537.
49. Yurtkuran A. (2019). An Improved Electromagnetic Field Optimization for the Global Optimization Problems, Computational Intelligence and Neuroscience, 2019, Article ID 6759106.

Prof. Olympia Roeva, Ph.D.
Email: olympia@biomed.bas.bg

Olympia Roeva received M.Sc. Degree (1998) and Ph.D. Degree (2007) from the Technical University – Sofia. At present she is a Professor at the Institute of Biophysics and Biomedical Engineering – Bulgarian Academy of Sciences. She has more than 200 publications, among those 10 books and book chapters, with more than 1000 citations. Her current scientific interests are in the fields of modelling, optimization and control of biotechnological processes, metaheuristic algorithms, intuitionistic fuzzy sets and generalized nets.

Assoc. Prof. Dafina Zoteva, Ph.D.
Email: dafinaz@fmi.uni-sofia.bg

Dafina Zoteva has a M.Sc. Degree in Bio- and Medical Informatics (2010) from Sofia University and Ph.D. Degree (2021) from the Institute of Biophysics and Biomedical Engineering at the Bulgarian Academy of Sciences. Currently, she is an Associate Professor at the Faculty of Mathematics and Informatics at Sofia University. She has more than 50 publications. Her scientific interests are in the fields of metaheuristic algorithms, intuitionistic fuzzy sets and generalized nets.